We are IntechOpen, the world's leading publisher of Open Access books Built by scientists, for scientists

6,900
Open access books available

185,000
International authors and editors

200M
Downloads

Our authors are among the

154
Countries delivered to

TOP 1%
most cited scientists

12.2%
Contributors from top 500 universities



WEB OF SCIENCE™

Selection of our books indexed in the Book Citation Index in Web of Science™ Core Collection (BKCI)

Interested in publishing with us?
Contact book.department@intechopen.com

Numbers displayed above are based on latest data collected.
For more information visit www.intechopen.com



Chapter

Influence of the Doping Ion Nature and Content on Defect Creation Processes under the Effect of Ionizing Radiation in Aluminoborosilicate Glasses

Eugenia Malchukova

Abstract

Effects of ionizing irradiation on defect creation processes have been studied in rare earth (RE)-doped (RE = Sm, Gd, Eu, Ce, Nd) aluminoborosilicate glass with use of the electron paramagnetic resonance (EPR) and optical spectroscopy. As a function of RE ion nature, we observe that doping significantly influences the nature of the defects produced during irradiation and more specifically the relative proportions between hole and electron defect centers. Strong decrease of defect production efficiency under ionizing radiation independence on both the RE doping content and on the relative stability of the RE different oxidation states is also clearly revealed. The results could be explained by dynamical reversible trapping of the electron-hole pairs produced during irradiation on the different RE charge states as well as by RE segregation and pre-existing defects speciation in ABS glass structure.

Keywords: borosilicate, glasses, EPR, luminescence, irradiation, defects

1. Introduction

Irradiation effects are an active research field in amorphous silica (aSiO2) due to many technological applications requiring a good maintenance of transparency (e.g. fibers, laser optics and radioactive environments) [1–4]. Indeed for aSiO2, the optical properties are controlled by the nature and the content of defect produced during an ionizing radiation (laser, X, γ, electrons) [5–7]. Different works using Electron Paramagnetic Spectroscopy (EPR) and optical absorption have shown that two different defects production processes occur during ionizing irradiation. The first process called intrinsic defects production [8–10] is correlated to Si–O bonds breaking leading to well-known paramagnetic E′ and Non-Bridging Oxygen Hole Centers (NBOHC) with self-trap excitons acting as possible precursors [11–13]. Peroxy radicals (POR) paramagnetic defect can also be produced with intrinsic process by the displacement of oxygen into an interstitial position like Frenkel defects [12, 14]. The second defect creation process is called “extrinsic” and is correlated to the presence of different impurities (H, Cl, Transition metals, Rare earth, ...) inside

IntechOpen

aSiO2 materials [8, 15–18]. In that case, the nature of different possible irradiation paramagnetic defects produced (E′, NBOHC, and POR) does not differ but an higher defect production efficiency is observed associated to saturation processes of defect content depending on impurities nature and content, respectively [19]. Defects production processes in aSiO2 are therefore mainly controlled by the nature and the content of the different impurities.

For more complex oxide glass compositions, the presence of network modifiers ions (Na^+, K^+, Ca^{2+}) and other network formers ions (B^{3+}, Al^{3+}) stabilizes with an high efficiency different hole trap like Boron-Oxygen Hole Center (BOHC) [20, 21], Aluminum-Oxygen Hole Center (AlOHC) [22] or Hole trapped defects on Non-Bridging Oxygen (NBO) called HC1, HC2 centers [23, 24]. In addition, the literature shows that the content of electron trap defects like E′ centers and equivalent defects closed to B^{3+} (BEC center) and Al^{3+} ions are generally much more lower than hole trap defects content for all oxide glass compositions including silica. Electron trapping on glass impurities like Hydrogen, alkaline, Transition Metals (TM), or Rare Earth (RE) ions could explain differences between the content of hole and electron trapped defects produced during exposure to ionizing radiation [7, 15]. In general for oxide glasses like borosilicate, silicate, and aluminosilicate, the nature and content of different paramagnetic defects observed by EPR spectroscopy will depend on the relative proportion of different network formers (Si^{4+}, Al^{3+}, and B^{3+}) and on network modifiers contents introduced inside the oxide glass. In case of aluminoborosilicate (ABS) glasses studied in this work, the nature and proportion of different paramagnetic defects have been previously determined using the simulation of EPR spectra of different β-irradiated borosilicate glass samples [25].

Doping processes of oxide glasses with rare earth (RE) ions influence a lot the nature and the content of different paramagnetic defects produced during exposure to ionizing radiation. In case of Sm- [26], Gd- [27], and Yb- [28] doped borosilicate glass compositions, the first effect of doping is the decrease of total paramagnetic defect contents produced during irradiation to one integrated dose. Moreover for Fe-doped soda-lime glasses [29] and Cr-doped silicate glasses [30], a complete disappearance of the different paramagnetic defects is observed for doping level around 1 mol. %. Associated to the decrease of paramagnetic defects production efficiency with the doping ion content, the decrease of different structural changes under irradiation detected by Raman spectroscopy [29, 30], (increase of polymerization and the molecular oxygen production, and decrease of Si–O–Si average angle) are also observed at integrated dose higher than 10^9 Gy. Structural changes in glasses under the effect of ionizing radiation are mainly controlled by alkaline mobility in both network modifiers and charge compensator positions [31]. This result shows therefore strong relationships between the nature and contents of doping ions, irradiation defects creation processes, and the structural changes due to ionizing radiation exposure in oxide glasses.

However, these previous studies have mainly focused on the modification of the total paramagnetic defect concentration produced during ionizing radiation as a function of the doping ion nature and content. The goal of this chapter is to systematically present the paramagnetic irradiation defect creation processes in rare earth-doped oxide glasses. First, the influence of RE doping ion nature on the relative paramagnetic defect proportion observed by EPR spectroscopy in the same ABS glass composition will be considered. Then, the influence of both doping ion content and integrated radiation dose on the nature, content, and relative proportion of the different paramagnetic defects produced during ionizing radiation will be considered also. It is known, that the optical spectroscopy is most useful in cases where EPR techniques are not applicable and for diamagnetic defects. Also, transmission and luminescence experiments will be carried out in order to provide additional information

on RE doping effect on ABS glass structure. This approach could improve our knowledge about defect creation processes under irradiation for ion doped oxide glasses. For that purpose, different RE-doped ABS glasses (RE = Sm, Gd, Eu, Ce, and Nd where the RE doping level between 0.1 and 1 mol. %) have been irradiated to different doses between 10^5 and 2×10^9 Gy using a Van de Graaff accelerator.

2. Experimental part

Rare earth-doped ABS glasses were prepared by adding to the base glass with the following composition—59.77% SiO_2, 4.00% Al_2O_3, 22.41% B_2O_3, 12.12% Na_2O, and 1.70% ZrO_2 (in mol. %)—different amounts of doping ions. The doping content of RE oxide considered in this work is shown in **Table 1**. The dried mixed powders were heated at 750°C for 10 h in air in a Pt crucible and melted at 1500°C for 2 h, then quenched on a copper plate. Before cutting, annealing at 500°C for 1–2 h was necessary to remove the internal stress. Samples were polished on a hand grinding wheel with a silicon carbide abrasive having the average grain size of 10 μm (1000 grain) to achieve the average thickness of 0.56 ± 0.05 mm. Each glass was analyzed by X-ray diffraction, in order to confirm the amorphous characteristics of the glass.

All glasses were β-irradiated with 2.5 MeV electrons (10 μA) provided by a Van de Graaff accelerator (LSI, Palaiseau, France) at different integrated doses from 10^6 to 2×10^9 Gy. The used sample thickness made it possible to obtain uniform irradiation on the entire glass volume. EPR measurements were conducted at room temperature on a X band (ν = 9.420 GHz) EMX Brücker EPR spectrometer using a 100 kHz field modulation, 3×10^{-4} Tesla of amplitude modulation and an applied microwave power of 1 mW. The EPR spectra of all irradiated RE-doped ABS glasses have been normalized to the same receiver gain and to a 100 mg sample weight. Paramagnetic defects total content has been estimated by the area under the defect absorbance EPR spectrum. A maximum error of 10% has been considered in this work taking into account uncertainties in the irradiated glass samples weight measurement, the sample positioning inside spectrometer cavity and defect absorbance EPR spectrum area computation or EPR line intensity measurement. The optical transmission spectra were measured on an Agilent Varian Cary 5000 spectrophotometer in 1 nm steps in the range of 200–1500 nm. The photoluminescence was analyzed by a SHAMROCK spectrograph F5303 mm: 150 lines/mm grating and a 400 mm slit combined with an ANDOR Istar (Andor Company, Belfast, U.K.) intensified charge coupled device. The 266 nm wavelength pulses width of around 8 ns and laser repetition rate of 10 Hz of an INDI Nd:YAG pulsed laser spectra physics were used for the PL excitation. The laser beam is transported via two mirrors, two lenses, and three diaphragms to the sample center with a final diameter of 2 mm. The pulse

Rare earth	mol%
Gd_2O_3	0.1; 0.2; 0.5; 1
Sm_2O_3	0.1; 0.2; 0.5; 1
Eu_2O_3	0.1; 0.2; 0.5; 1
Nd_2O_3	0.1; 0.2; 0.6; 1
CeO_2	0.2; 0.4; 1.2; 2

Table 1.
RE doping concentration.

energy on the sample was ~2 mJ/pulse. The spectral measurements were carried out using different delay time (d) and gate width (G).

3. EPR spectra of RE-doped ABS glass: b-irradiation dose effect

Without doping, the nature of the different defects produced by ionizing radiation has been previously studied in the non-doped ABS glass composition irradiated with 2.5 MeV electrons by the simulation of the EPR spectra of irradiated samples annealed at different temperatures [25]. The EPR of the non-doped ABS glass irradiated at 1.3×10^8 Gy is presented in **Figure 1**. The main component of these EPR spectra is associated to the hyperfine structure with 11B (I = 3/2). The defect is called the Boron-Oxygen Hole Center (BOHC) (g1 = 2.0029, g2 = 2.0115, and g3 = 2.0500) and it is attributed to a hole trap on an oxygen link to a boron atom [21]. The second hole center for this glass composition that can be observed at high annealing temperature is the peroxy radical (Si–O–O°) named Oxy defect (g1 = 2.0024, g2 = 2.0110, and g3 = 2.0439) in the literature for silicate glasses [22]. The last hole center determined by the simulation of the EPR spectra for this glass composition is the HC1 center attributed to a hole trapped on a non-bridging oxygen in the vicinity of alkaline ion. Finally, the EPR line around g = 2.0011 is an electron trap and is attributed to the well-known E′ center [11].

Figure 1 presents the EPR spectra recorded at room temperature of the non-doped and 0.1 mol% RE-doped ABS glasses (RE = Sm, Gb, Eu, Nd, and 0.2 mol% Ce) irradiated with 2.5 MeV electrons (integrated dose of 1.3×10^8 Gy). First, It can be observed

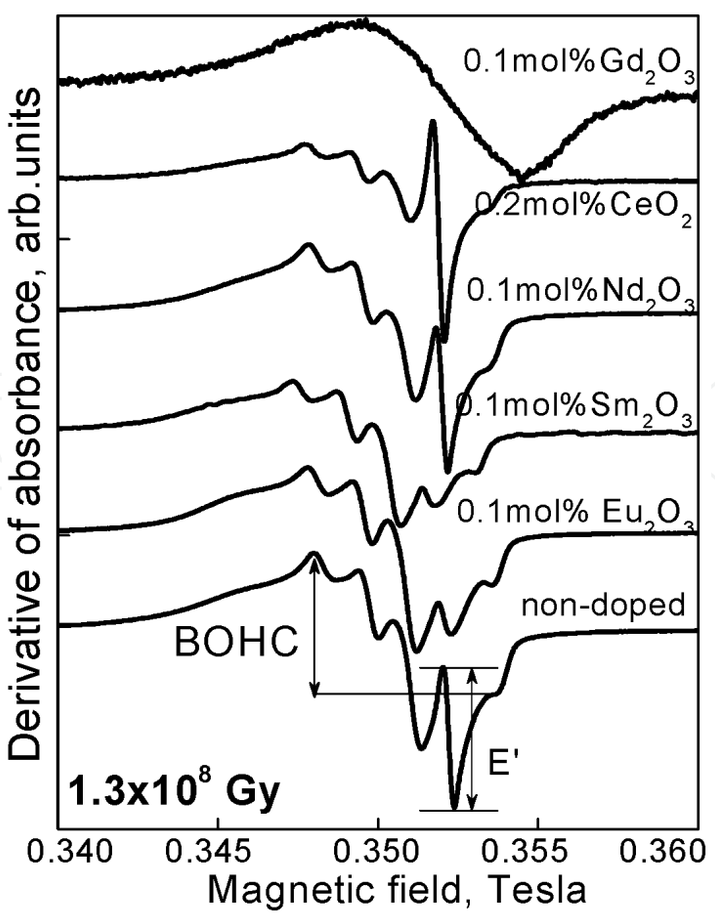


Figure 1.
X band EPR spectra of the lowest RE-doped ABS glasses (RE = Gd, Sm, Eu, Ce, and Nd) irradiated at 1.3×10^8 Gy.

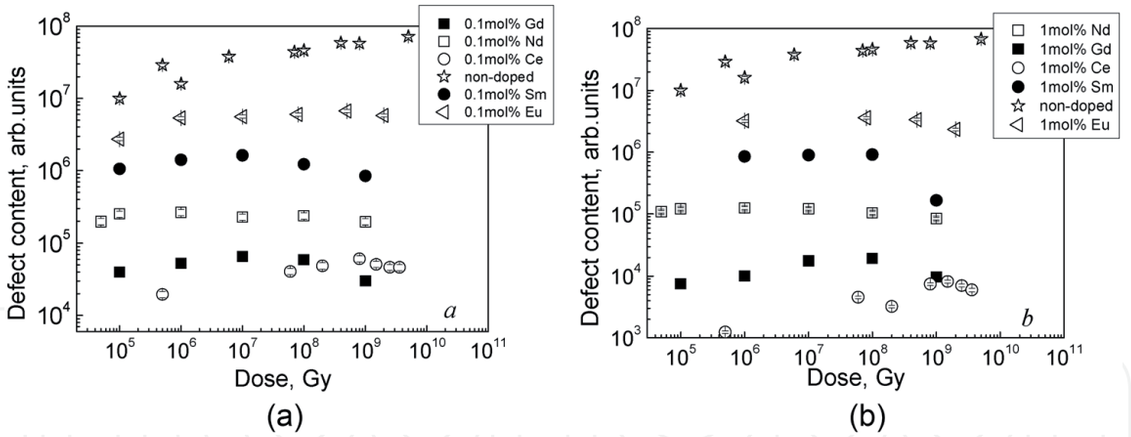


Figure 2.
Evolution of EPR defects content as a function of integrated dose for the lowest: (a) and the highest; (b) concentration of RE doping of β–irradiated ABS glass (RE = Gd, Sm, Eu, Ce, and Nd).

clearly on that figure that RE doping at low level (0.1 mol%) influences significantly both the amount of defect produced during irradiation and their relative proportions. More specifically, a decrease of the different hole centers (HC) is analyzed depending on the nature of the doping ion ([HC]Eu > [HC]Sm > [HC]Nd > [HC]Ce). This effect is maximum for 0.2 mol% Ce-doped glasses where the content of hole centers is drastically decreasing in comparison with the non-doped glass composition. For E′ center detected at g = 2.0011 in the non-doped ABS glass, a strong increase as a function of the RE doping ion nature is observed ([E′]Eu < [E′]Sm < [E′]Nd < [E′]Ce). However, for all ABS glass compositions studied, the quantity of electron defect centers (E′) remains smaller than the hole defect centers (BOHC, OXY, HC_1) showing therefore the presence of other mechanisms acting as traps for the electrons produced during irradiation.

Evolution of the total paramagnetic defect content for all RE-doped glasses (RE = Sm, Gd, Eu, Nd, and Ce) as a function of the integrated dose is presented in logarithmic scales on **Figure 2** for two different RE doping levels: 0.1 and 1 mol%, on **Figure 2a** and **b**, respectively.

For non-doped ABS glass, the total defect concentration is increasing with the integrated dose. This behavior can be correlated with extrinsic and/or intrinsic defect creation processes under the effect of ionizing radiation [8]. Two effects can be observed in **Figure 2a** and **b**. First, the decrease of the defect produced during irradiation at one integrated dose depending on the nature of the RE doping ion. The second effect is saturation behavior of the defect content as a function of the integrated dose associated to a decrease of the defect content at higher doses for all RE-doped glasses. We can therefore conclude that glass doping processes play an important role on defect creation processes under the effect of ionizing radiation.

4. EPR spectra of RE-doped ABS glass: RE concentration effect

The influence of RE content on defect production under irradiation is shown in **Figure 3a** and **b** for two different integrated doses. For all RE doping considered in this work, the defect content is decreasing as a function of the RE doping content inside the glass but with different efficiency depending on the RE nature.

In addition, the relative proportions between the different paramagnetic defects observed by EPR spectroscopy are modified by both the nature of the RE ion and also its content in the host glasses. These effects can be seen on **Figures 4–7** showing the normalized EPR spectra of irradiated (1.3×10^8 Gy) glass samples doped with

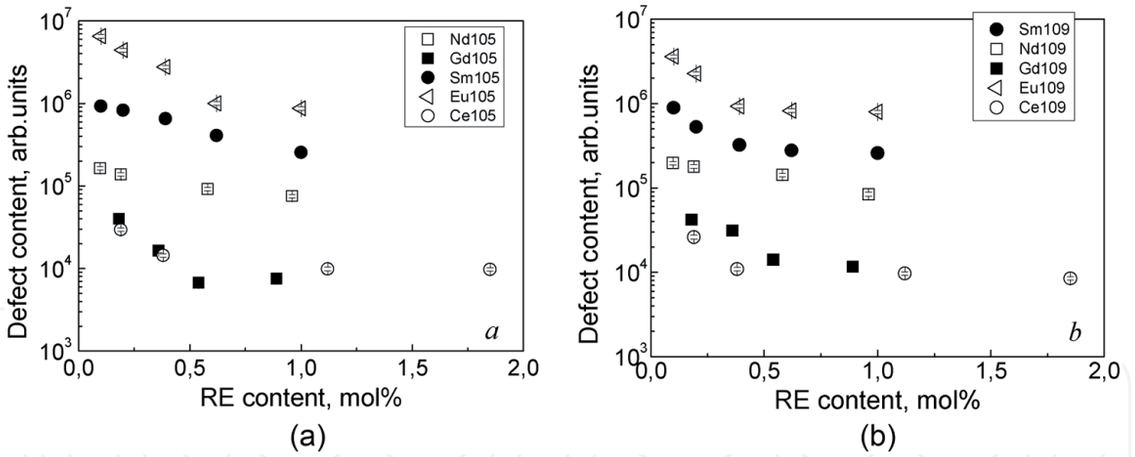


Figure 3.
Evolution of EPR defects concentration as a function of the RE doping ion content in ABS glasses β–irradiated at 6.5 × 10⁶: (a) and 2.6 × 10⁹ Gy; (b) RE = Gd, Sm, Eu, Ce, and Nd.

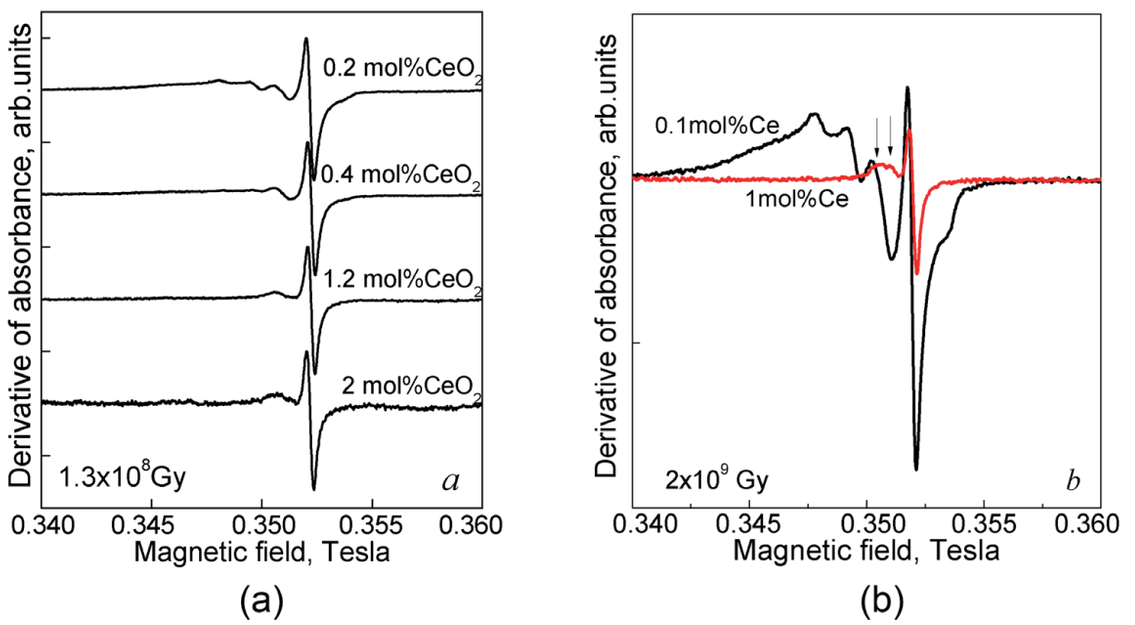


Figure 4.
X band EPR spectra recorded at room temperature of 0.2, 0.4, 1.2, and 2 mol.% CeO_2-doped ABS glass irradiated at 1.3 × 10⁸ Gy (the EPR spectra have been normalized to E′ EPR line intensity): (a) and X band EPR spectra of 0.2 and 2 mol.%CeO_2-doped ABS glass irradiated at 2 × 10⁹ Gy (b).

Ce, Eu, Sm, and Nd ions, respectively. From the **Figure 4a** one can see the strongest influence of doping on defect production in Ce-doped glasses: a huge decreased of different holes centers (BOHC, OXY, HC_1) in the defect EPR spectrum is observed starting from the lowest doping level considered in this work (0.2 mol.% of CeO_2). The BOHC center becomes undetectable in the EPR spectra at Cerium doping levels higher than 0.2 mol.% and the hole defects remaining in the EPR spectra is the OXY and HC1 centers as it is shown in **Figure 4b** for the Ce-doped ABS glass irradiated at 2 × 10⁹ Gy (arrows in **Figure 4b**). This effect is more pronounced in the case of the highest doses (more than 10⁹ Gy). From **Figure 5a** and **b**, it can be concluded that Ce doping strongly inhibits the defect production observed by EPR spectroscopy and in addition stops the different holes defects production under the effect of ionizing radiation. BOHC defect is also detected.

When comparing these results with Eu-doping in the same ABS glass composition, similar effects of doping ion content on defect production efficiency are observed by EPR spectroscopy (**Figure 5**). But in the case of Eu-doping, a

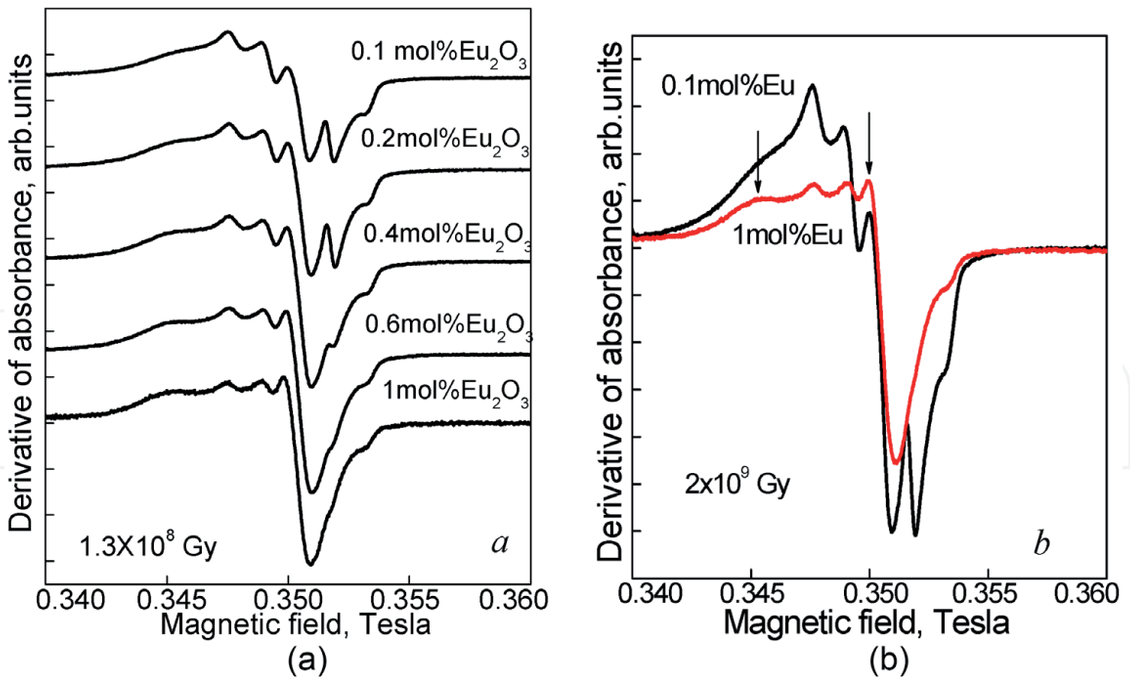


Figure 5.
X band EPR spectra recorded at room temperature of 0.1, 0.2, 0.5, and 1 mol.% Eu_2O_3-doped ABS glass irradiated at 1.3 × 10^8 Gy (the EPR spectra have been normalized to BOHC EPR line intensity) (a) and X band EPR spectra of 0.1 and 1 mol.% Eu_2O_3-doped ABS glass irradiated at 2 × 10^9 Gy (b).

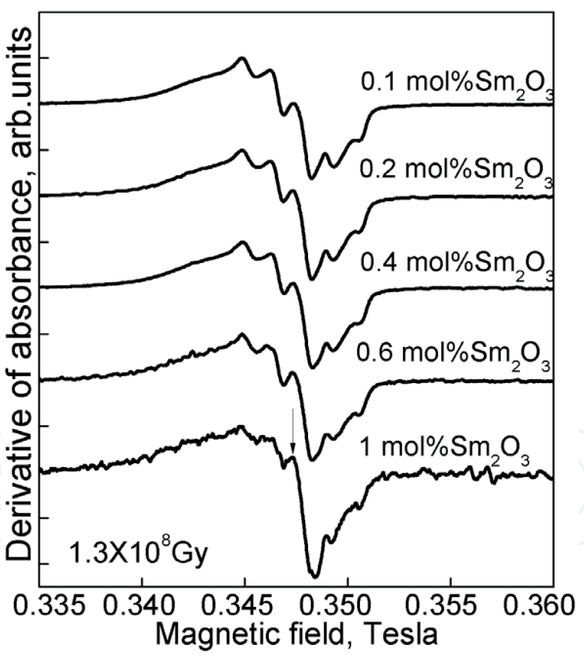


Figure 6.
X band EPR spectra recorded at room temperature of 0.1, 0.2, 0.4, 0.6, and 1 mol.% Sm_2O_3-doped ABS glass irradiated at 1.3 × 10^8 Gy (the EPR spectra have been normalized to BOHC EPR line intensity).

strong decrease of E′ centers contribution in the defect EPR spectra can be seen (**Figure 5a**). The E′ center becomes undetectable in the EPR spectra at Europium doping levels higher than 0.6 mol.% and the hole defects re-arrangement in the EPR spectra between OXY and BOHC centers can be observed. The highest irradiation dose results in more re-arrangement of hole defects as can be seen from **Figure 5b** (arrows in the **Figure 5b**). The influence of Sm- (**Figure 6**) and Nd- (**Figure 7**) doping contents are weaker than for Ce-doped ABS glasses for both the decrease in

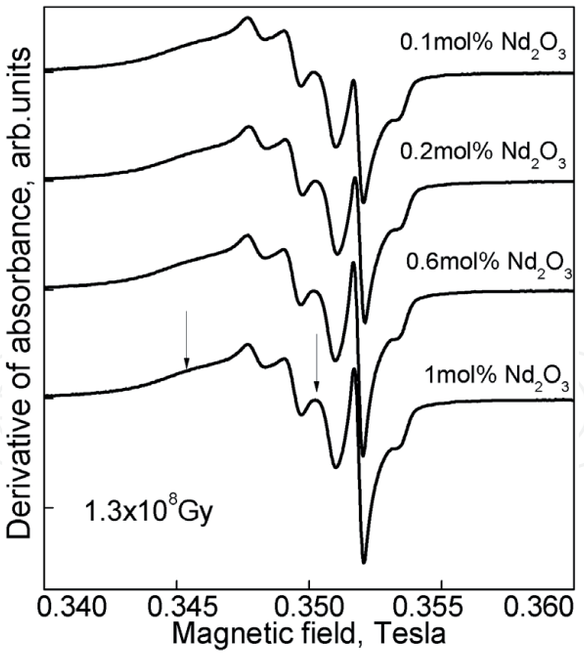


Figure 7.
X band EPR spectra recorded at room temperature of 0.1, 0.2, 0.6, and 1 mol.% Nd_2O_3-doped ABS glass irradiated at 1.3 × 10^8 Gy (the EPR spectra have been normalized to BOHC EPR line intensity).

defect production efficiencies and the changes in the relative proportions of defects composing the EPR spectra of these irradiated glass samples. However, a decrease in the relative proportion of the different defect holes centers (BOHC, Oxy, HC_1) for the different Nd-doped ABS glasses (**Figure 7**) can be observed.

This effect could also be correlated to the evolution analyzed for Ce-doped ABS glasses. The changes of the relative proportions of defect as a function of Sm-doping content in ABS glasses (**Figure 6**) show mainly the decrease of E′ defect component in the EPR spectra. Associated to this decrease, an increase in the relative proportion of OXY center relative to relative to BOHC defect is also detected.

The experiments testify that glass doping processes can influence the proportion between different defects produced during irradiation compared to the non-doped glass composition. This change has been usually correlated to the capacity of the doping ion to act as a trap for the holes and electrons produced during irradiation. Eu^{3+} ions are known to be good electron traps and one can observe on **Figures 1** and **5a** the strong decrease of the E′ proportion relatively to the non-doped ABS glasses. Sm^{3+} ion can also be reduced during the exposure to ionizing radiation but with a weaker efficiency than Eu^{3+} ions, this effect is also observed on the decrease of the relative proportion of E′ centers in the defect EPR spectra (**Figures 1** and **6**). By contrast, Ce^{3+} ions produced during irradiation or during the synthesis of Ce-doped glasses is a well-known hole traps [32, 33]. So these ions (Eu^{3+}, Sm^{3+}, and Ce^{3+}) can therefore compete with the hole trap defects production as represented for Eu-, Sm-, and Ce-doped ABS glasses. Relative proportion between hole and electron defects in the EPR spectra of irradiated RE-doped ABS glasses can be considered as a parameter for the estimation of the interaction of doping ions with the ionizing radiation.

However, other parameters can influence the nature of the different defects produced during irradiation and more specifically the speciation of the RE ions inside the host glasses. Indeed, some authors like Li and coworkers have studied the solubility and the environment of gadolinium in borosilicate glass compositions [34, 35]. They show that this RE ion is preferentially located in the vicinity of boron network former. According to literature, this RE ion is not therefore homogeneously distributed inside glass. This result influence strongly the EPR spectra of irradiated

Gd-doped ABS glasses (**Figure 1**) where the defect EPR spectrum is broad and not resolved due to dipole-dipole interaction between BOHC centers and paramagnetic Gd^{3+} ions. This effect could also explain the evolution of the EPR spectra of Eu-doped ABS glasses (**Figures 5a** and **5b**) as a function of doping ion content. This figure shows both decrease of the relative proportion of BOHC and E′ centers contributions in the defect EPR spectra. As Eu ions can be considered as an electron trap, the changes in relative proportion between OXY and BOHC defects shown in **Figure 6a** could show Eu speciation in the vicinity of boron network former. In order to understand the RE doping influence on defect production under ionizing radiation, Magic Angle Spinning Nuclear magnetic resonance spectroscopy (MAS NMR) of ^{11}B could be a way for studying as a function of RE nature in glasses, their possible influence on BOHC defect production.

The second influence of RE doping inside ABS glasses concerns the efficiency of defect production as a function of both nature of the doping ions and its content (**Figure 3**). The decrease of paramagnetic defects concentration can be due to the fact that the electron-hole pairs produced during ionizing radiation can support dynamical balance between the two different charge states of RE ions ($RE^{n+1} + (h°/e^-) => RE^n + h° => RE^{n+1}$ or $RE^n + (h°/e^-) => RE^{n+1} + e^- => RE^n$). Therefore, this process efficiency of defect production can be correlated to the stability of different oxidation states for different RE ions. Moreover, it is known that increase of the dopant content up to 1 mol.% in highly irradiated (3×10^9 Gy) Fe^{3+}- and Cr^{3+}-doped glasses may lead to the complete disappearance of the defect EPR spectrum [29, 30]. But it is necessary to take into consideration the Fe^{3+} (Cr^{3+}) ions dipole-dipole interaction effect on the defect EPR spectrum. In that case, the disappearance or decrease of defect EPR spectrum in the doped glasses as a function of doping ion content could also be associated with heterogeneous speciation of defects produced during exposure to ionizing radiation in the vicinity of doping ions.

For all RE doping ABS glasses considered in this work, saturation behavior of defect EPR spectra is analyzed as the function of the integrated dose. This result is explained by the strong efficiency of the dynamical trapping processes of electron-hole pairs on different redox states of RE doping ions with respect to the defect production efficiency under the effect of ionizing radiation in this ABS glass. In addition in **Figure 2a** and **b**, the defect content is decreasing in some cases at integrated doses higher than 5×10^8 Gy. Structural changes were observed for irradiated glass samples at doses around 10^9 Gy due to the effect of ionizing radiation and might be correlated to the alkaline migration [31]. The decrease of defect content at higher doses could therefore show an important role of precursor defect on the alkaline migration processes leading to glass structural changes.

5. Optical spectra: Effect of RE doping on defect band

The available structural information on defects in glass was derived mainly from the results of electron paramagnetic resonance (EPR) spectrometry. It should be noticed that this method is directly applicable only to the subclass of defects which are paramagnetic. A more formidable problem is the pre-existing intrinsic point defects, which are not of paramagnetic nature. Examples of intrinsic diamagnetic defects believed to occur in silica glass include neutral oxygen vacancies (≡Si-Si≡), two-coordinated silicone (O–Si–O–), and peroxy linkages (≡Si–O–O–Si≡) [5]. The most common extrinsic defects are associated with hydroxyl and chloride impurities [16]. It is obvious that the defect designation in multicomponent glasses is extremely complex. Thus, the combined information obtained from EPR- and

optical (absorption and photoluminescence (PL)) spectra can give an additional data on the structure of the glasses and of the pre-existing/radiation-induced imperfections. Often some defects can provide large EPR signal but the induced optical extinction (transmission loss) is very low and vice versa.

A compendium of EPR/optical correlations was reported in the literature [36, 37] and pointed to the most likely origins of many defect-related optical absorption bands in the visible, ultraviolet, and vacuum-ultraviolet spectral regions. But the assignment of the bands is still controversial in some cases. In this section, some preliminary results on optical study of pristine and irradiated ABS glass doped with RE ions are presented.

Non-doped ABS glass has high ultraviolet transmission. No significant defect generation was detected (**Figures 8** and **9**, black line) in pristine glass. Only small transmission losses in the UV spectral region 230–240 nm were found (**Figure 9**) to be, it seems, connected with oxygen-deficient centers formed on the basis of silicon [15]. Oxygen-deficient centers (ODC, "oxygen vacancies") are the natural type of intrinsic defects in non-stoichiometric silicon dioxide [38]. By the existence of these types of defect in silica optical and luminescent properties are defined as described in [38, 39]. The dominating opinion has been still to consider vacancies of bridging oxygen atoms as the precursors of radiation E′ centers [38, 39]. Thus, ODCs play the key role in E′ center formation and their concentrations in glass. In irradiated ABS glass (BK7 or Duran type) the silicon and boron related electron centers (SiEC and BEC are considered to be responsible for this absorption) [37]. Also after irradiation with high dose (more than 10^9 Gy) some additional transmission losses can be observed in visible part of the spectra at ~360 and 600 nm (**Figures 9** and **10**, red line) caused by intrinsic radiation defect generation. In [37], these bands are attributed to the BOHC defects in ABS glass.

Photoluminescence (PL) was detected in both pristine and irradiated ABS glasses. As aforementioned in the spectra of pristine ABS glass the ODCs are displayed in the form of an absorption band at 230–240 nm. According to [15] ODSs emission is observed at 280 and 450 nm. Under excitation of forth harmonic

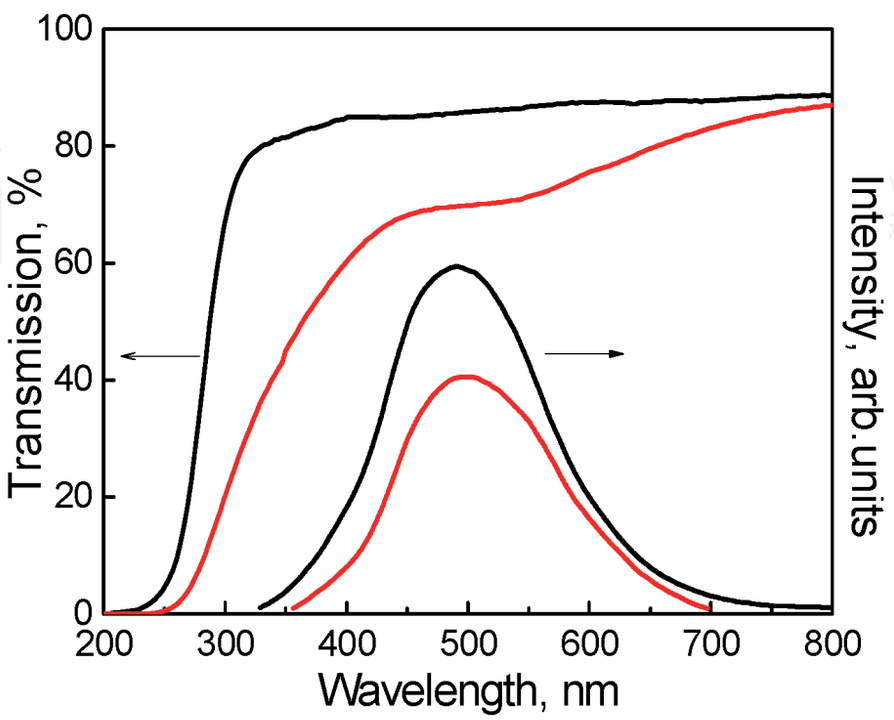


Figure 8.
Transmission and PL spectra of pristine and irradiated (10^9 Gy) non-doped ABS glasses.

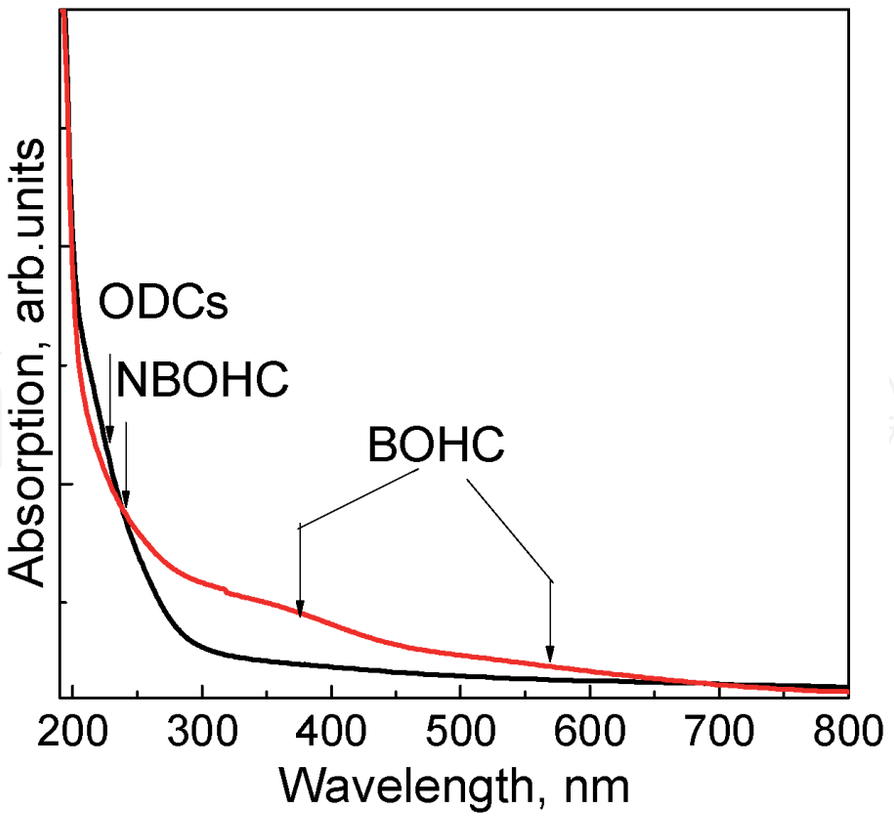


Figure 9.
Absorption spectra of pristine and irradiated (10^9 Gy) non-doped ABS glasses.

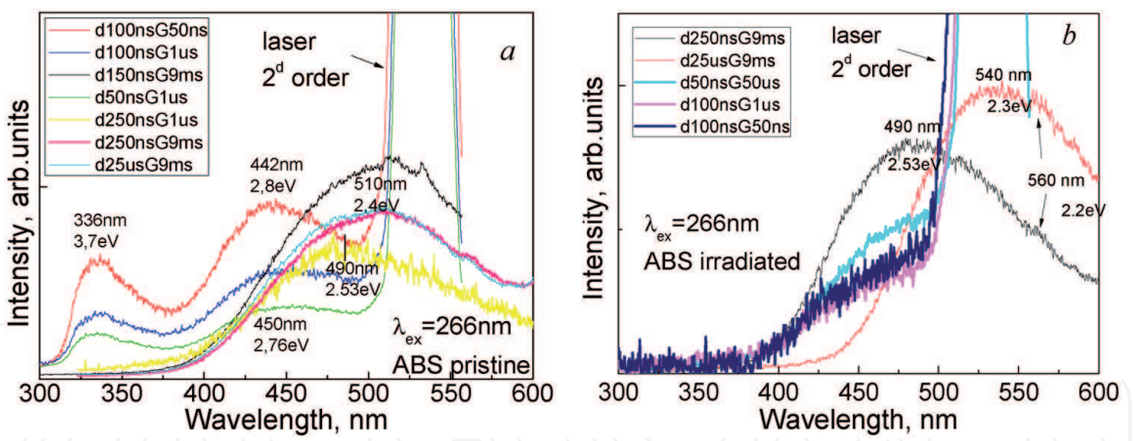


Figure 10.
Time-resolved luminescence spectra of pristine: (a) and irradiated (10^9 Gy); (b) non-doped ABS glasses measured at different gate width and time delay (λ_{exc} = 266 nm Nd:YAG laser).

of Nd:YAG laser (266 nm) we can see only the appearance of broad PL band at ~500 nm for both pristine (**Figure 8**, black line) and β-irradiated glass samples (**Figure 8**, red line). It should be noticed that the position, shape, width, and intensity of this band are different for these two glass samples (**Figure 8**).

Time-resolved luminescence measurements carried out with laser excitation (266 nm) revealed the variety of pre-existing point defects in ABS glass (**Figure 10a**) most of them are not identified and described in the literature on our opinion. For one exception: the band at 442 nm can be attributed to ODC which is consistent with data [15]. Especially taking into account that β-irradiation terminates this emission completely as well as two others at 336 and 510 nm. At the same time the new one (540 nm (5.3 eV); perhaps attributed to NBOHC [36]) is arising

but emission band at 490 nm is still observed with higher intensity in irradiated ABS glass (**Figure 10b**). It should be marked here that the band at 336 nm can be also assigned to the ODCs since as it is indicated in [15] "Si ODCs in the silica glass network are an ensemble of defects such as 'oxygen vacancies', which differ in local structural environment, i.e., in the symmetry and strength of the local crystalline fields around the ODC." That is why the ODCs to be characterized by a rather wide variety of spectral characteristics.

The incorporation of RE ions into the ABS glass matrix affects its optical properties. The evolution of optical characteristics is discussed in frame of the non-bridging oxygen formation in the glass structure, as well as color centers as a function of the nature of the RE element. By increasing the number of Nd (Gd) ions in ABS glass, it is possible to observe a decrease in the number of non-bridging oxygen per silicon tetrahedron in the glass studied which is confirmed by the estimate of the optical band gap and the Raman spectroscopy data. The presence of two charge states of multivalent Eu and Ce ions having absorption in the UV region complicates the consideration of the effect of the processes on the observed change in the optical band gap energy. The effect of irradiation results in color centers content increase (observed as more intense brown coloration of the irradiated glass) in the following sequence, Nd < Gd < Sm = Eu < Ce. This evolution is reflected on the optical band gap narrowing [40]. **Figure 11** presents transmission and PL spectra of the highly Sm-doped (1 mol.%) pristine and irradiated ABS glass. Some transmission losses can be observed for pristine glass from **Figure 12**: firstly, due to the presence of Sm^{3+} ions in glass structure (sharp lines in the spectra) and secondly, due to the presence of ODCs (similar to the non-doped ABS glass, see **Figure 8**). The emission spectra consist of the well-known bands belonging to the Sm^{3+}/Sm^{2+} ions and the broad band around 500 nm, attributed to the ODCs: intensity of this band decreases significantly by β-irradiation (**Figure 11**).

The transmission spectra of Gd-doped ABS glass do not change significantly in comparison with non-doped glass except the fact that no prominent transmission losses are observed at 360 and 600 nm in irradiated glass (**Figure 12**). Emission of ODCs are located in the visible part of PL spectra at ~500 nm as it was seen before

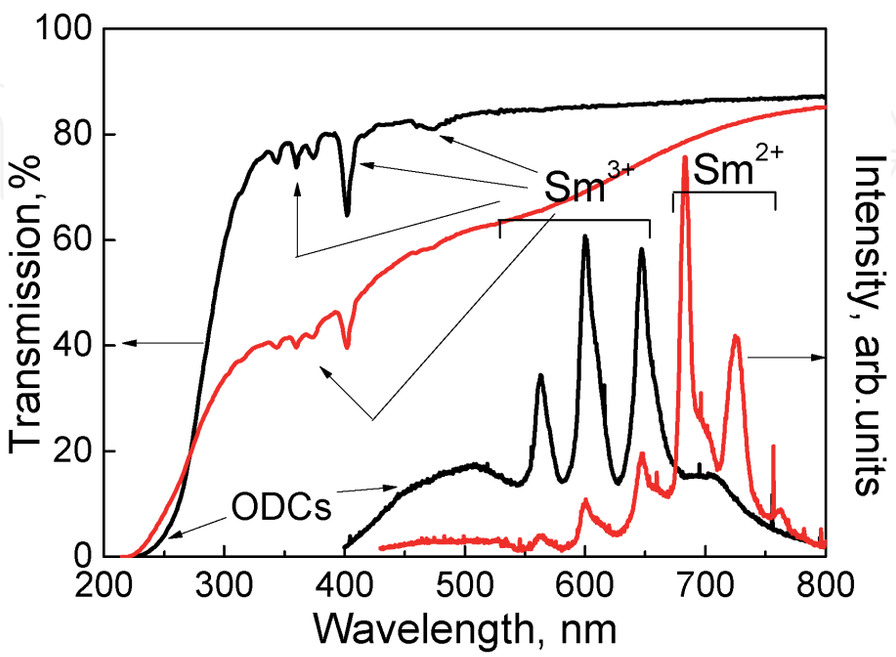


Figure 11.
Transmission and PL spectra of pristine and irradiated (10^9 Gy) Sm-doped ABS glasses.

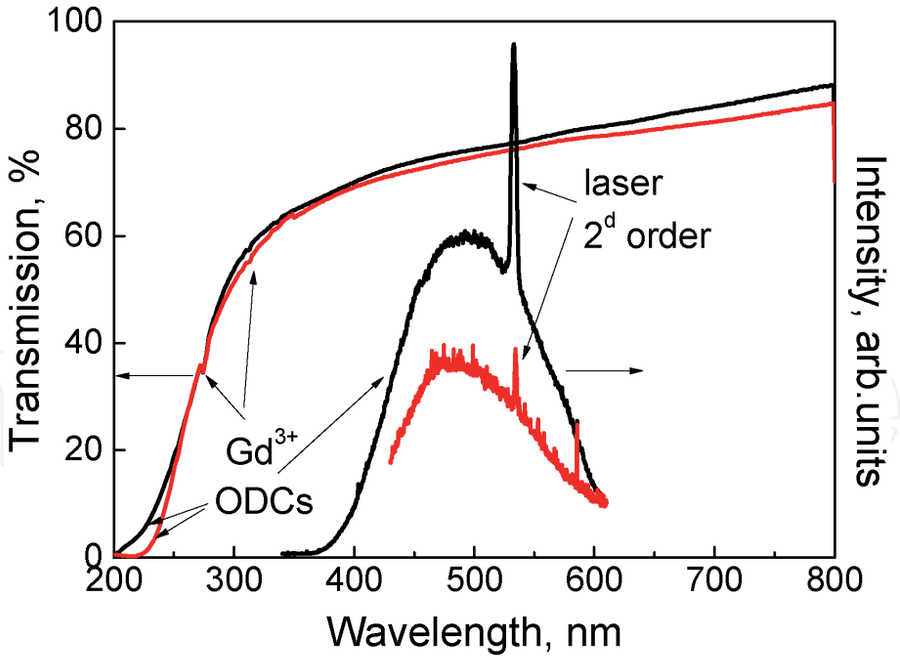


Figure 12.
Transmission and PL spectra of pristine and irradiated (10^9 Gy) Gd-doped ABS glasses.

for non-doped and Sm-doped ABS glass (**Figures 8** and **11**, respectively). It was shown [41] that this emission can also be excited by third harmonic of Nd:YAG laser (355 nm). Unfortunately, no information about ODCs optical characteristics could be obtained in Eu- or Ce-doped ABS glasses because of strong Eu^{2+}, $Ce^{3+}/^{4+}$ absorption in the UV studied spectral region [40]. It is clearly seen that the absorption and PL characteristics of ODCs in non-doped ABS glass, as well as in glass doped with Sm or Gd ions, are analogous to each other with the exception of unresolved PL bands structure in case of doping (**Figure 13**).

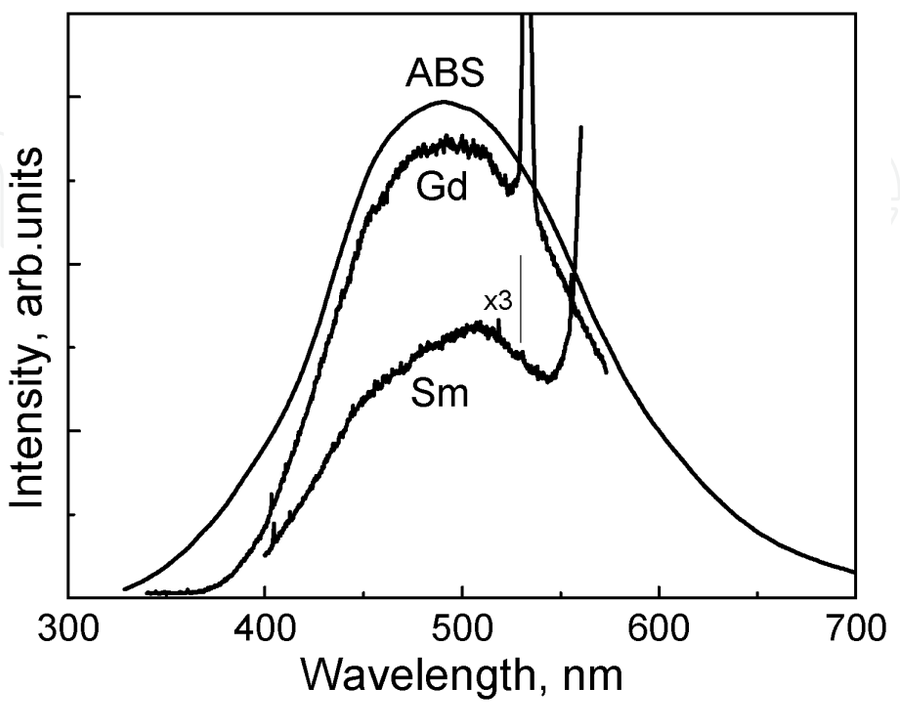


Figure 13.
Evolution of the defect emission band on RE dopant nature.

It was natural to suppose that we have similar types of defect. But for the moment it is not absolutely clear whether these ODCs have essentially different structure or whether they are the same vacancies with distorted environment. Moreover, the modified shape of the PL band can be consistent with the assumption about the effect of segregation of defects and impurities that can influence the variations of the spectral characteristics of the ODCs. In the previous section, the relative increase in the proportion of peroxy radicals (Si–O–O°: Oxy defects) with the Eu concentration as well of the Oxy and the HC_1 (Si–O Na^+) centers with Ce concentration (**Figures 4** and **5**) was reported. Probably it means that the structural model of the OXY and HC_1 centers tightly depends on the structural model of the ODC and it is still open for discussion. As to our point of view observed experimental facts can be most naturally explained by segregation of impurities and defects in the glass network. The effect of selective incorporation of a RE dopant into the glass due to the heterogeneous glass structure, leading to a RE concentration dependent dopant displacement as well as concentration dependent optical and physical-chemical glass properties which was firstly mentioned in the 1970 [42]. Then phase-separation model was suggested in order to explain structural evolution of RE-doped borosilicate glass [34, 35].

Analysis of the results presented allowed to draw a conclusion that due to RE speciation in the ABS glass structure and heterogeneous distribution between different environments RE doping affects strongly defect production (firstly, pre-existing defects). Additional studies on RE concentration dependent time-resolved luminescence ABS glass might be required.

6. Summary and outlook

The presented study has shown significant changes in defect creation processes under ionizing radiation in ABS glasses as a function of the nature and the content of different rare earth-doping ions (RE = Sm, Gd, Eu, Ce, and Nd). We observe first that doping processes influence significantly the nature of the different defect produced during ionizing radiation and more specifically the ratio between hole and electron defect centers observed by EPR spectroscopy. The specific role of RE doping ion acting as a hole or an electron trap could control the population of different defects produced during irradiation. The second result of doping is a strong decrease in defect production efficiency under the effect of ionizing radiation depending on both the RE doping content in the glass and on the relative stability of the RE different oxidation states. This result could be explained by dynamical reversible trapping of the electron-hole pairs produced during irradiation on the RE ions as well as by RE segregation and pre-existing defects speciation in ABS glass structure.

In order to understand the RE doping influence on defect production under the effect of ionizing radiation, Magic Angle Spinning Nuclear magnetic resonance spectroscopy (MAS NMR) of ^{11}B could be a way for studying as a function of RE nature in glasses and their possible influence on BOHC defect production.

Acknowledgements

I would like to thank Thierry Pouthier and Vincent Métayer for their contribution during external β-irradiation experiments. I do appreciate also to Dr. B. Boizot for stimulating my interest in this field and for pointing to my attention several interesting experimental problems as well as for many enlightening discussions.

DOI: http://dx.doi.org/10.5772/intechopen.92317

IntechOpen

IntechOpen

Author details

Eugenia Malchukova
Ioffe Institute, Russian Academy of Sciences, St. Petersburg, Russia

*Address all correspondence to: e.malchukova@mail.ioffe.ru

IntechOpen

© 2020 The Author(s). Licensee IntechOpen. This chapter is distributed under the terms of the Creative Commons Attribution License (http://creativecommons.org/licenses/by/3.0), which permits unrestricted use, distribution, and reproduction in any medium, provided the original work is properly cited. CC BY

References

[1] Pacchioni G, Skuja L, Griscom DL, editors. Defects in SiO_2 and Related Dielectrics: Science and Technology. Dordrecht: Kluwer Academic Publishers; 2000. DOI: 10.1007/978-94-010-0944-7. 615p

[2] Grillanda S, Singh V, Raghunathan V, Morichetti F, Melloni A, Kimerling L, et al. Gamma radiation effects on silicon photonic waveguides. Optics Letters. 2016;**41**(13):3053-3056. DOI: 10.1364/OL.41.003053

[3] Lisovskyy IP, Voitovych MV, Voitovych VV, Khacevich IM. Influence of radiation on the luminescence of silicon nanocrystals embedded into SiO_2 film. Journal of Nanomaterials. 2016;**2016**:9674741. DOI: 10.1155/2016/9674741

[4] Alessia A, Richard N, Martin-Samos L, De Michelea V, Giacomazzi L, Agnello S, et al. Overview of radiation induced point defects in silica-based optical fibers. Physical Review. 2019;**4**:100032(18). DOI: 10.1016/j.revip.2019.100032

[5] Griscom DL. Optical properties and structure of defects in silica glass. Journal of the Ceramic Society of Japan. 1991;**99**:923-942

[6] Du Q, Huang Y, Ogbuu O, Zhang W, Li J, Singh V, et al. Gamma radiation effects in amorphous silicon and silicon nitride photonic devices. Optics Letters. 2017;**42**(3):587-590. DOI: 10.1364/OL.42.000

[7] Skuja L, Hirano M, Hosono H, Kajihara K. Defects in oxide glasses. Physica Status Solidi C. 2005;**2**(1):15-24. DOI: 10.1002/pssc.200460102

[8] Imai H, Hirashima H. Intrinsic- and extrinsic-defect formation in silica glasses by radiation. Journal of Non-Crystalline Solids. 1994;**179**:202-213. DOI: 10.1016/0022-3093(94)90698-X

[9] Devine RAB, Arndt J. Correlated defect creation and dose-dependent radiation sensitivity in amorphous SiO_2. Physical Review B. 1989;**39**(8):5132-5138. DOI: 10.1103/physrevb.39.5132

[10] Devine RAB, Arndt J. Defect pair creation through ultraviolet radiation in dense, amorphous SiO_2. Physical Review B. 1990;**42**(4):2617-2620. DOI: 10.1103/physrevb.42.2617

[11] Weeks RA. The many varieties of E' centers: A review. Journal of Non-Crystalline Solids. 1994;**179**:1-9. DOI: 10.1016/0022-3093(94)90680-7

[12] Griscom DL, Friebele EJ. Fundamental defect centers in glass: 29Si hyperfine structure of the nonbridging oxygen hole center and the peroxy radical in a-SiO_2. Physical Review B. 1981;**2**(8):4896-4898. DOI: 10.1103/PhysRevB.24.4896

[13] Imai H, Arai K, Isoya J, Hosono H, Abe Y, Imagawa H. Generation of E' centers and oxygen hole centers in synthetic silica glasses by gamma irradiation. Physical Review B. 1993;**48**(2):3116-3123. DOI: 10.1103/physrevb.48.3116

[14] Zhang L, Mashkov VA, Leisure RG. Multiple interconversions of the E' and oxygen-hole defect centers in high-purity amorphous silica during anneal-interrupted x irradiation. Physical Review Letters. 1995;**74**(9):1605-1608. DOI: 10.1103/PhysRevLett.74.1605

[15] Amossov AV, Rybaltovsky AO. Radiation color center formation in silica glasses: A review of photo- and thermo-chemical aspects of the problem. Journal of Non-Crystalline Solids. 1994;**179**:226-234. DOI: 10.1016/0022-3093(94)90700-5

[16] Skuja L, Kajihara K, Hirano M, Hosono H. Hydrogen-related radiation

defects in SiO_2-based glasses. Nuclear Instruments and Methods in Physics Research B. 2008;**266**(12-13):2971-2975. DOI: 10.1016/j.nimb.2008.03.150

[17] Elsts E, Rogulis U, Bulindzs K, Smits K, Zolotarjovs A, Trinkler L, et al. Studies of radiation defects in cerium, europium and terbium activated oxyfluoride glasses and glass ceramics. Optical Materials. 2015;**41**:90-93. DOI: 10.1016/j.optmat.2014.10.042

[18] Uklein AV, Popov AS, Lisnyak VV, Zaderko AN, Linnik RP, Boldyrieva OY, et al. Probing of the oxygen-related defects response in Nd:phosphate glass within self-action of the laser radiation technique. Journal of Non-Crystalline Solids. 2018;**498**:244-251. DOI: 10.1016/j.jnoncrysol.2018.06.024

[19] Mashkov VA, Austin WR, Zhang L, Leisure RG. Fundamental role of creation and activation in radiation-induced defect production in high-purity amorphous SiO_2. Physical Review Letters. 1996;**76**(6):2926-2929. DOI: 10.1103/PhysRevLett.76.2926

[20] Griscom DL. E.S.R. studies of radiation damage and structure in oxide glasses not containing transition group ions: A contemporary overview with illustrations from the alkali borate system. Journal of Non-Crystalline Solids. 1973;**13**:251-285. DOI: 10.1016/0022-3093(74)90095-7

[21] Kordas G. On the structure of the BOHC in the borosilicate and boro-phosphosilicate glasses. Journal of Non-Crystalline Solids. 2005;**351**:2348-2360. DOI: 10.1016/j.jnoncrysol.2005.06.010

[22] Dutt DA, Higby PL, Griscom DL. An electron spin resonance study of X-irradiated calcium aluminosilicate glasses. Journal of Non-Crystalline Solids. 1991;**130**:41-521. DOI: 10.1016/0022-3093(91)90154-X

[23] Kordas G, Camara B, Oel HJ. Electron spin resonance studies of radiation damage in silicate glasses. Journal of Non-Crystalline Solids. 1982;**50**:79-95. DOI: 10.1016/0022-3093(82)90202-2

[24] Griscom DL. Electron spin resonance studies of trapped hole centers in irradiated alkali silicate glasses: A critical comment on current models for HC_1 and HC_2. Journal of Non-Crystalline Solids. 1984;**64**:229-247. DOI: 10.1016/0022-3093(84)90220-5

[25] Boizot B, Petite G, Ghaleb D, Calas G. Radiation induced paramagnetic centers in nuclear glasses by EPR spectroscopy. Nuclear Instruments and Methods in Physics Research B. 1998;**141**:580-584. DOI: 10.1016/S0168-583X(98)00102-5

[26] Malchukova E, Boizot B, Petite G, Ghaleb D. Optical properties and valence state of Sm ions in aluminoborosilicate glass under β-irradiation. Journal of Non-Crystalline Solids. 2007;**353**: 2397-2402. DOI: 10.1016/j.jnoncrysol.2007.04.003

[27] Malchukova E, Boizot B, Ghaleb D, Petite G. β-Irradiation effects in Gd-doped borosilicate glasses studied by EPR and Raman spectroscopies. Journal of Non-Crystalline Solids. 2006;**352**(4):297-303. DOI: 10.1016/j.jnoncrysol.2005.11.003

[28] Ollier N, Planchais R, Boizot B. EPR study of Yb-doped irradiated glasses. Nuclear Instruments and Methods in Physics Research B. 2008;**266**(12-13): 2854-2858. DOI: 10.1016/j.nimb.2008.03.129

[29] Olivier FY, Boizot B, Ghaleb D, Petite G. Raman and EPR studies of β-irradiated oxide glasses: The effect of Iron concentration. Journal of Non-Crystalline Solids. 2005;**351** (12-13):1061-1066. DOI: 10.1016/j.jnoncrysol.2005.01.018

[30] Boizot B, Olivier FY, Petite G, Ghaleb D. Blocking of alkaline migration under ionizing irradiation in Cr-doped oxide glasses. Nuclear Instruments and Methods in Physics Research B. 2008;**266**(12-13):2966-2970. DOI: 10.1016/j.nimb.2008.03.149

[31] Boizot B, Ollier N, Olivier F, Petite G, Ghaleb D, Malchukova E. Irradiation effects in simplified nuclear waste glasses. Nuclear Instruments and Methods in Physics Research B. 2005;**240**(1-2):146-151. DOI: 10.1016/j.nimb.2005.06.105

[32] Qiu J, Sugimoto N, Iwabuchi Y, Hirao K. Photostimulated luminescence in Ce^{3+}-doped silicate glasses. Journal of Non-Crystalline Solids. 1997;**209**:200-203. DOI: 10.1016/S0022-3093(96)00644-8

[33] Vedda A, Nikl M, Fasoli M, Mihokova E, Pejchal J, Dusek M, et al. Thermally stimulated tunneling in rare-earth-doped oxyorthosilicates. Physical Review B. 2008;**78**:195123(8). DOI: 10.1103/PhysRevB.78.195123

[34] Li L, Li H, Quian M, Strachan DM. Gadolinium solubility in peralkaline borosilicate glasses. Journal of Non-Crystalline Solids. 2001;**283**:237-245. DOI: 10.1016/S0022-3093(01)00480-X

[35] Li H, Su Y, Li L, Strachan DM. Raman spectroscopic study of gadolinium(III) in sodium-aluminoborosilicate glasses. Journal of Non-Crystalline Solids. 2001;**292**:167-176. DOI: 10.1016/S0022-3093(01)00878-X

[36] Skuja L. Optically active oxygen-deficiency-related centers in amorphous silicon dioxide. Journal of Non-Crystalline Solids. 1998;**239**(1-3):16-48. DOI: 10.1016/S0022-3093(98)00720-0

[37] Ehrt D, Ebeling P. Radiation defects in borosilicate glasses. European Journal of Glass Science and Technology. Part A: Glass Technology. 2003;**44**(2):46-49

[38] Weeks RA. Paramagnetic resonance of lattice defects in irradiated quartz. Journal of Applied Physics. 1956;**27**(11):1376-1381. DOI: 10.1063/1.1722267

[39] Hosono H, Abe Y, Kinser DL, Weeks RA, Muta K, Kawazoe H. Nature and origin of the 5-eV band in SiO_2:GeO_2 glasses. Physical Review B. 1992;**46**:11445-11451. DOI: 10.1103/physrevb.46.11445

[40] Malchukova EV, Nepomnyashchikh AI, Boizot B, Terukov EI. Radiation effects and optical properties of aluminoborosilicate glass doped with RE ions. Glass Physics and Chemistry. 2018;**44**(4):356-363. DOI: 10.1134/S1087659618040090

[41] Mal'chukova EV, Nepomnyashchikh AI, Boizot B, Shamirzaev TS, Petite G. Luminescence of aluminoborosilicate glasses doped with Gd^{3+} ions. Physics of the Solid State. 2010;**52**(9):1919-1924. DOI: 10.1134/S1063783410090222

[42] Dmitryuk AV, Karapetyan GO, Maksimov LV. Activator segregation and its spectroscopic signatures. Zhurnal Prikladnoi Spektroskopii. 1975;**22**(1):153-182